Supplementary Material for

Achieving 1.2 fm/Hz$^{1/2}$ Displacement Sensitivity with Laser Interferometry in Two-Dimensional Nanomechanical Resonators: Pathways towards Quantum-Noise-Limited Measurement at Room Temperature

Jiankai Zhu[1#], Luming Wang[1#], Jiaqi Wu[1#], Yachun Liang[1], Fei Xiao[1], Bo Xu[1], Zejuan Zhang[1], Xiulian Fan[2], Yu Zhou[2*], Juan Xia[1*], and Zenghui Wang[1,3*]

[1] Institute of Fundamental and Frontier Sciences, University of Electronic Science and Technology of China, Chengdu, China

[2] School of Physics and Electronics, Hunan Key Laboratory of Nanophotonics and Devices, Central South University, Changsha, China

[3] State Key Laboratory of Electronic Thin Films and Integrated Devices, University of Electronic Science and Technology of China, Chengdu, China

[#]Equal contributing authors.

[*]Corresponding authors. Emails: yu.zhou@csu.edu.cn, juanxia@uestc.edu.cn, zenghui.wang@uestc.edu.cn

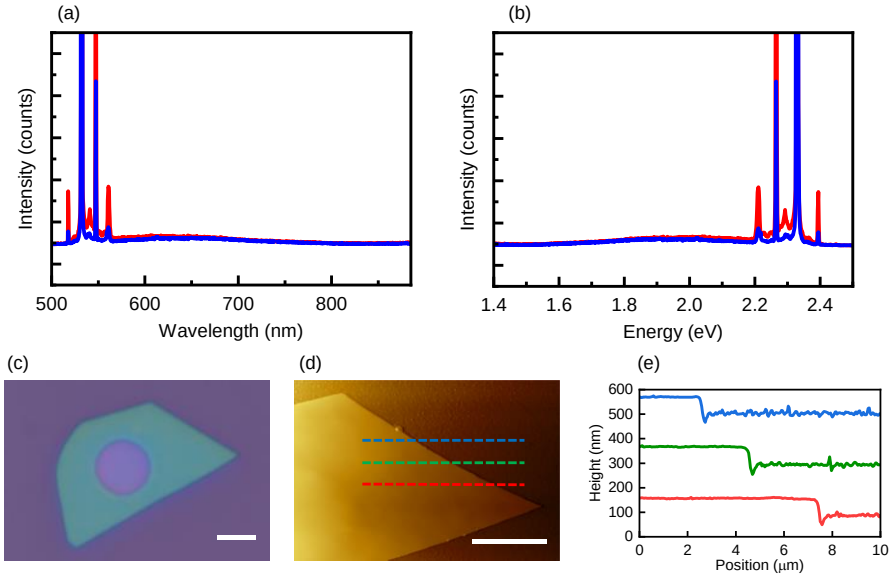

Fig. S1. Characterization of $CaNb_2O_6$ samples. (a-b) PL spectra of $CaNb_2O_6$ sample plotted in wavelength and energy. The absence of PL features is consistent with $CaNb_2O_6$ being a large-bandgap 2D material. (c) Optical image of a $CaNb_2O_6$ nanomechanical resonator, with a circular suspended area in the middle. (d) AFM image of a $CaNb_2O_6$ resonator. (e) Height traces extracted from the colored lines in (d), with measured step heights of 65.6, 73.3, and 68.5 nm. We use the average value (69.1 nm) as the device thickness. All scale bars: 5 μm.

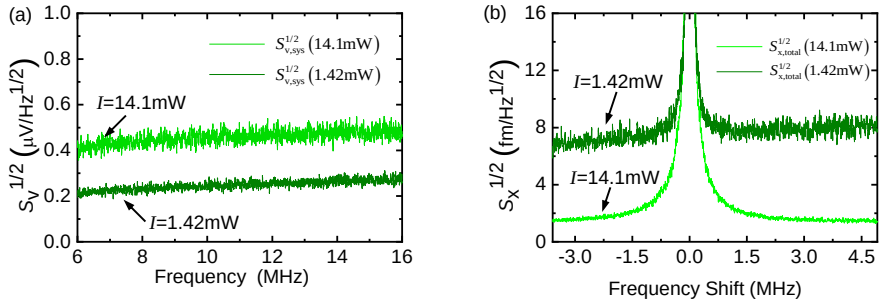

Fig. S2. Comparison of noise and SNR under different on-detector laser powers. (a) Measured noise under two different on-detector laser powers, plotted in voltage domain. Note that higher laser power leads to higher shot noise (and thus higher laser noise). (b) Measured thermomechanical noise under two different on-detector laser powers, plotted in displacement domain. Note that higher laser power leads to higher SNR.

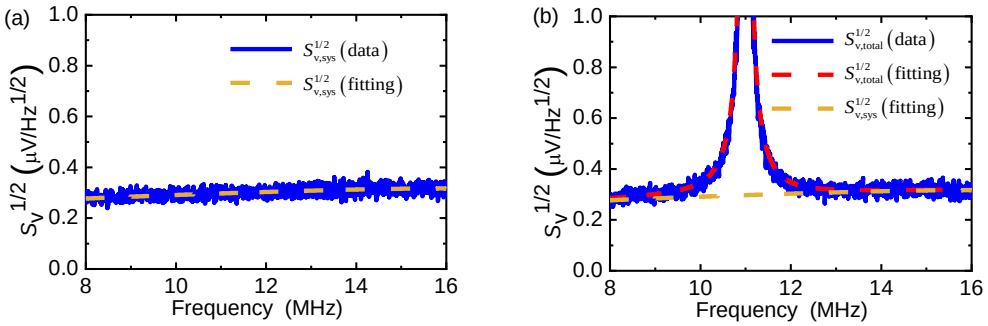

Fig. S3. Characterization of system noise floor. (a) Measured noise spectrum with the laser spot just off the resonator, and with laser power adjusted. (b) Measured noise spectrum of a $CaNb_2O_6$ resonator, showing the thermomechanical resonance peak. For measurements with large laser intensities, the thermomechanical resonance peak is sizable and thus requires a large measurement bandwidth (range of measurement frequency) in order to capture the entire resonance peak. In such cases the system noise background cannot simply be approximated as a constant or a linear function of frequency. We thus perform careful characterization of system noise by moving the laser spot just off the resonator to remove the thermomechanical resonance peak. Due to the difference in reflectance, we carefully adjust the laser intensity to obtain a noise spectrum off the device, shown in (a), which has about the same noise level as the off-resonance part of the on-device measurement, shown in (b). We then use a polynomial function of frequency to fit the off-device noise spectrum (dashed lines), as use this polynomial function in combination with a linear function is used in previous work [38, 47] as the noise floor of the measurement system $S_{v,sys}^{1/2}$ for subsequent fittings. This is also how the excess laser noise data (magenta curves in Fig. 2) is measured.

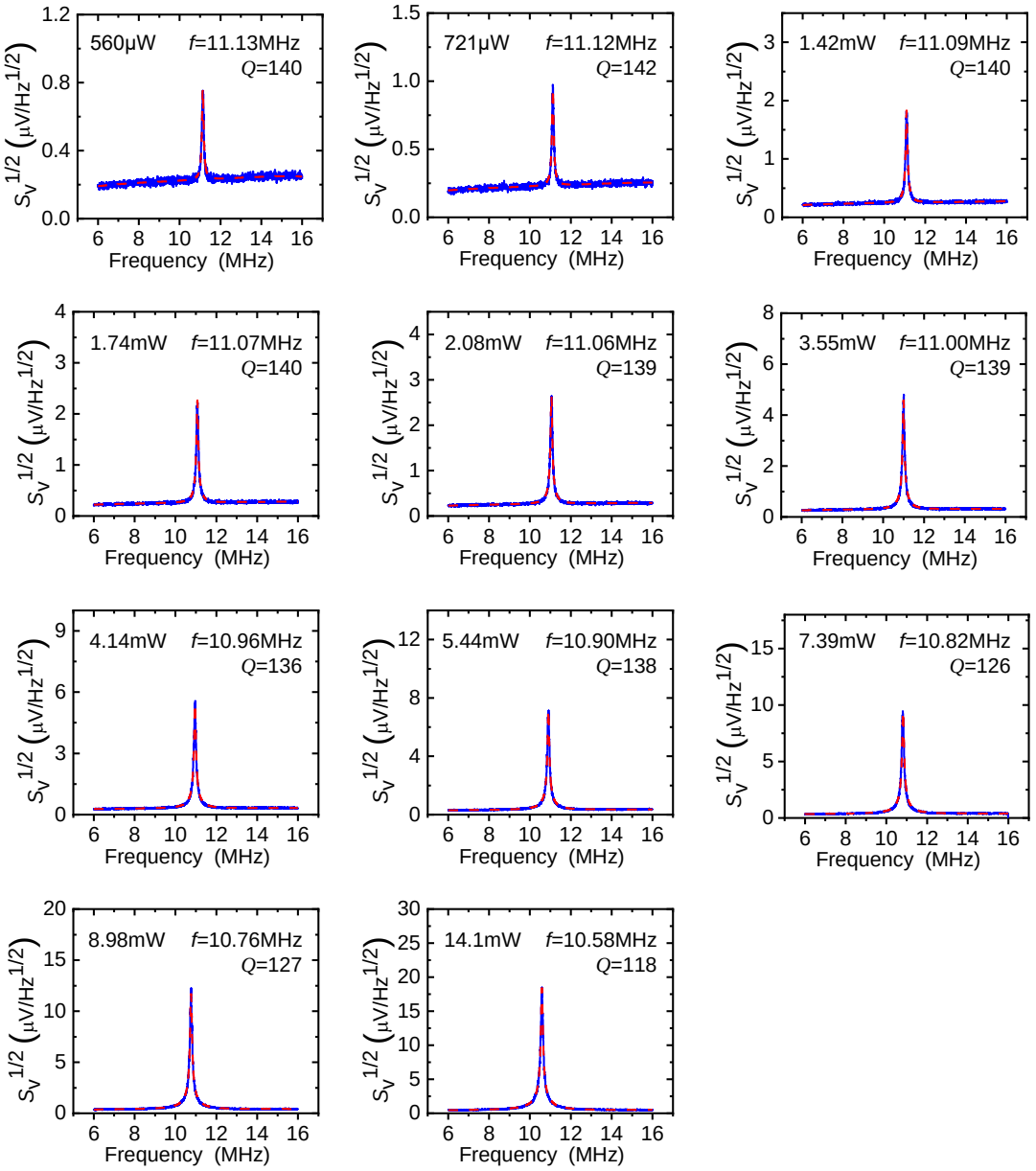

Fig. S4. Measured noise spectra in the $CaNb_2O_6$ resonator (69.1 nm thick) over a range of laser intensities. Note that the vertical scale is adjusted for each laser intensity value so that the thermomechanical resonance peak remains clearly visible. On-device laser intensity values are labeled in each panel. Both measured data (blue) and fitting (red) are shown, along with the resonance frequency and quality factor extracted from each fitting.

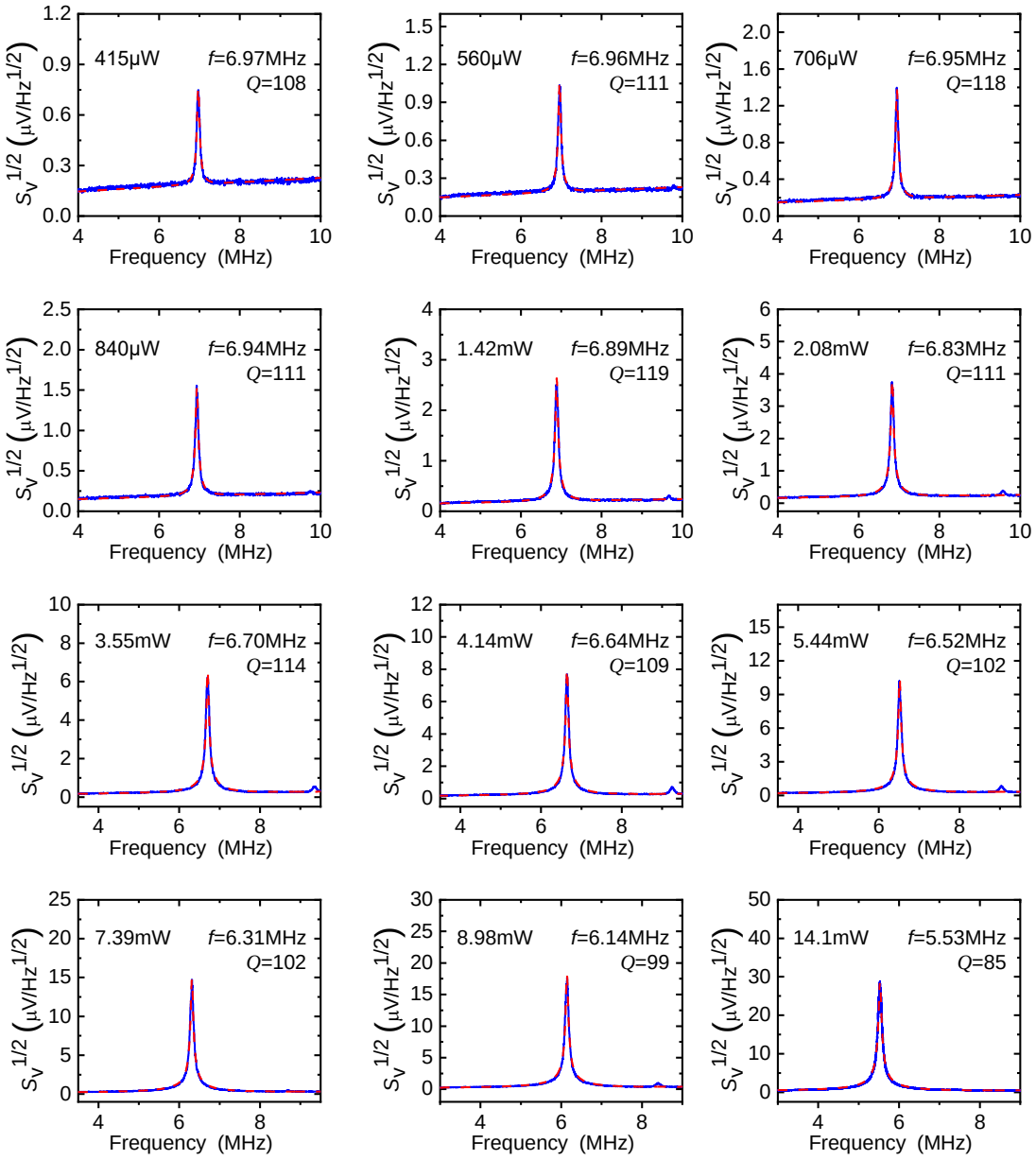

Fig. S5. Measured noise spectra in another $CaNb_2O_6$ resonator (44.8 nm thick) over a range of laser intensities. Note that the vertical scale is adjusted for each laser intensity value so that the thermomechanical resonance peak remains clearly visible. On-device laser intensity values are labeled in each panel. Both measured data (blue) and fitting (red) are shown, along with the resonance frequency and quality factor extracted from each fitting.

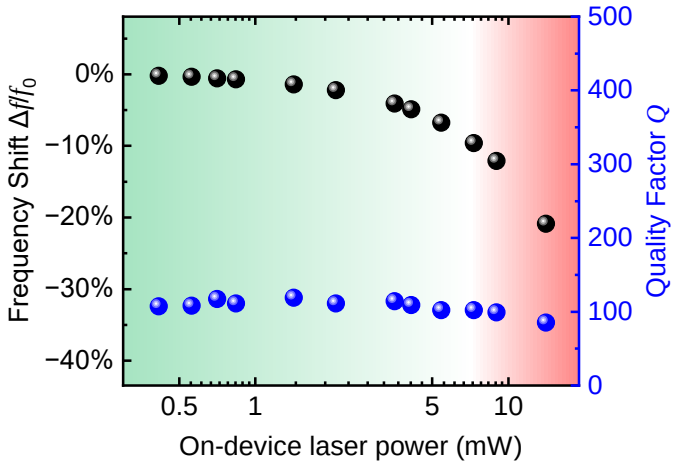

Fig. S6. Measured device resonance frequency (black) and quality factor (blue) under different levels of incident (on-device) laser power for the same device (44.8 nm thick) in Fig. S5.

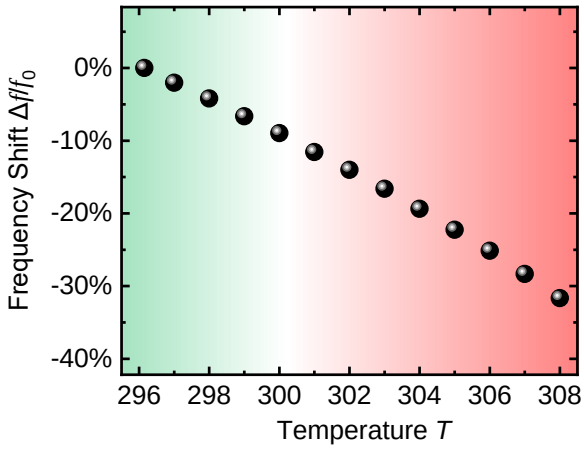

Fig. S7. TC*f* measurement for the same device (44.8 nm thick) in Fig. S5. The resonance measurement is performed in a cryostat, with an on-device laser power of 0.28 mW which does not heat the device. The device temperature is controlled by a temperature controller that controls a resistive heater near the end of the cooling head of the cryostat (no cooling power during the experiment), and read off from a silicon diode temperature sensor mounted near the heater. Both the heater and temperature sensor are close (within a few mm) to and have good thermal contact (using an all-metal sample holder) with the resonator device chip, which is mounted at the end of the cooling head.

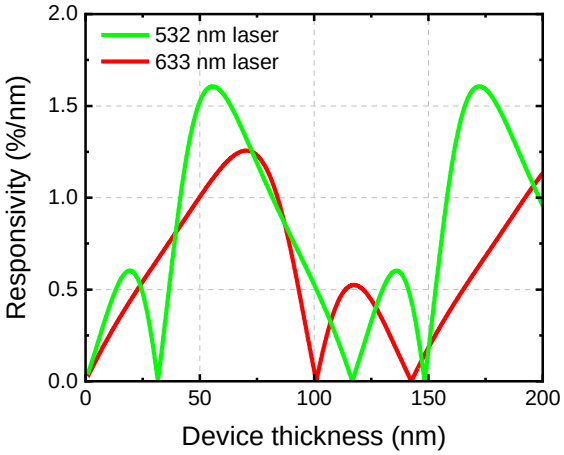

Fig. S8. Calculated displacement-to-reflectance responsivity for $CaNb_2O_6$ resonators under 532 nm and 633 nm illuminations as a function of $CaNb_2O_6$ thickness d_1. The device model is shown in Fig.1(a) inset of the Main Text. The reflectance R is calculated using the expression [36, 37]:

$$R(r,\theta)=\frac{I_{\text{interferometry}}}{I_{\text{incident}}}=\left|\frac{\boldsymbol{r}_1 e^{i(\boldsymbol{\phi}_1+\phi_2)}+\boldsymbol{r}_2 e^{-i(\boldsymbol{\phi}_1-\phi_2)}+\boldsymbol{r}_3 e^{-i(\boldsymbol{\phi}_1+\phi_2)}+\boldsymbol{r}_1\boldsymbol{r}_2\boldsymbol{r}_3 e^{i(\boldsymbol{\phi}_1-\phi_2)}}{e^{i(\boldsymbol{\phi}_1+\phi_2)}+\boldsymbol{r}_1\boldsymbol{r}_2 e^{-i(\boldsymbol{\phi}_1-\phi_2)}+\boldsymbol{r}_1\boldsymbol{r}_3 e^{-i(\boldsymbol{\phi}_1+\phi_2)}+\boldsymbol{r}_2\boldsymbol{r}_3 e^{i(\boldsymbol{\phi}_1-\phi_2)}}\right|^2,$$

where $\boldsymbol{r}_1$, $\boldsymbol{r}_2$, and $\boldsymbol{r}_3$ are reflection coefficients at the vacuum-$CaNb_2O_6$, $CaNb_2O_6$-vacuum, and vacuum-Si interfaces, respectively:

$$\boldsymbol{r}_1=\frac{n_{\text{vac}}-\boldsymbol{n}_{\text{MoS}_2}}{n_{\text{vac}}+\boldsymbol{n}_{\text{MoS}_2}},\quad \boldsymbol{r}_2=\frac{\boldsymbol{n}_{\text{MoS}_2}-n_{\text{vac}}}{\boldsymbol{n}_{\text{MoS}_2}+n_{\text{vac}}},\quad \boldsymbol{r}_3=\frac{n_{\text{vac}}-\boldsymbol{n}_{\text{Si}}}{n_{\text{vac}}+\boldsymbol{n}_{\text{Si}}},$$

and ϕ_1, ϕ_2 are the phase shifts when the light is traveling in different media:

$$\boldsymbol{\phi}_1=\frac{2\pi\boldsymbol{n}_{\text{MoS}_2}d_1}{\lambda},\quad \phi_2=\frac{2\pi n_{\text{vac}}d_2}{\lambda},$$

where λ is the wavelength of the laser. In the above equations, each d stands for the thickness, and each $\boldsymbol{n}$ stands for the complex index of refraction of the respective layers ($CaNb_2O_6$, vacuum gap, and silicon), with only n_{vac} being real value and equal to unity. Values used in the calculation are: Initial vacuum gap depth: d_2=290 nm; Vacuum: n_{vacuum}=1; Silicon [36]: $\boldsymbol{n}_{Si}$ = 4.15-0.044i (532nm) and 3.881-0.019i (633nm); $CaNb_2O_6$ [31]: $\boldsymbol{n}_{CaNb2O6}$ = 2.28-0.78×$10^{-5}i$ (532nm) and 2.22-0.87×$10^{-5}i$ (633nm). Displacement-to-reflectance responsivity is calculated by taking partial derivative of the reflectance function with respect to the vacuum gap depth, *i.e.*, $\partial R/\partial d_2$. The magnitude (without sign) of the responsivity value is plotted, as the sign does not affect the efficiency of signal transduction.

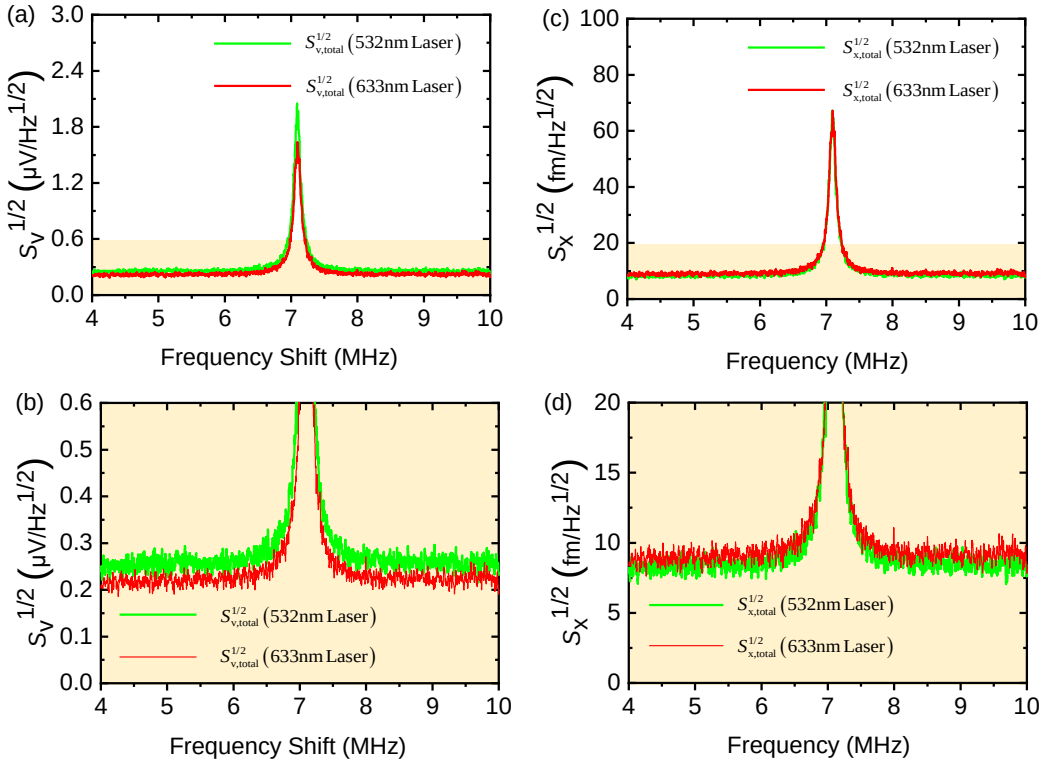

Fig. S9. Measurements of thermomechanical motion for the same device (44.8 nm thick) in Fig. S5, using 532 nm (green) and 633 nm (red) lasers. (a) Measured noise spectrum with on-device laser power of 1.5 mW, plotted in voltage domain. (b) Enlargement of the colored area in (a). Note that 532 nm laser leads to higher laser noise. (c) Measured noise spectrum with on-device laser power of 1.5 mW, plotted in displacement domain. (d) Enlargement of the colored area in (c). Note that 532 nm laser leads to higher SNR.

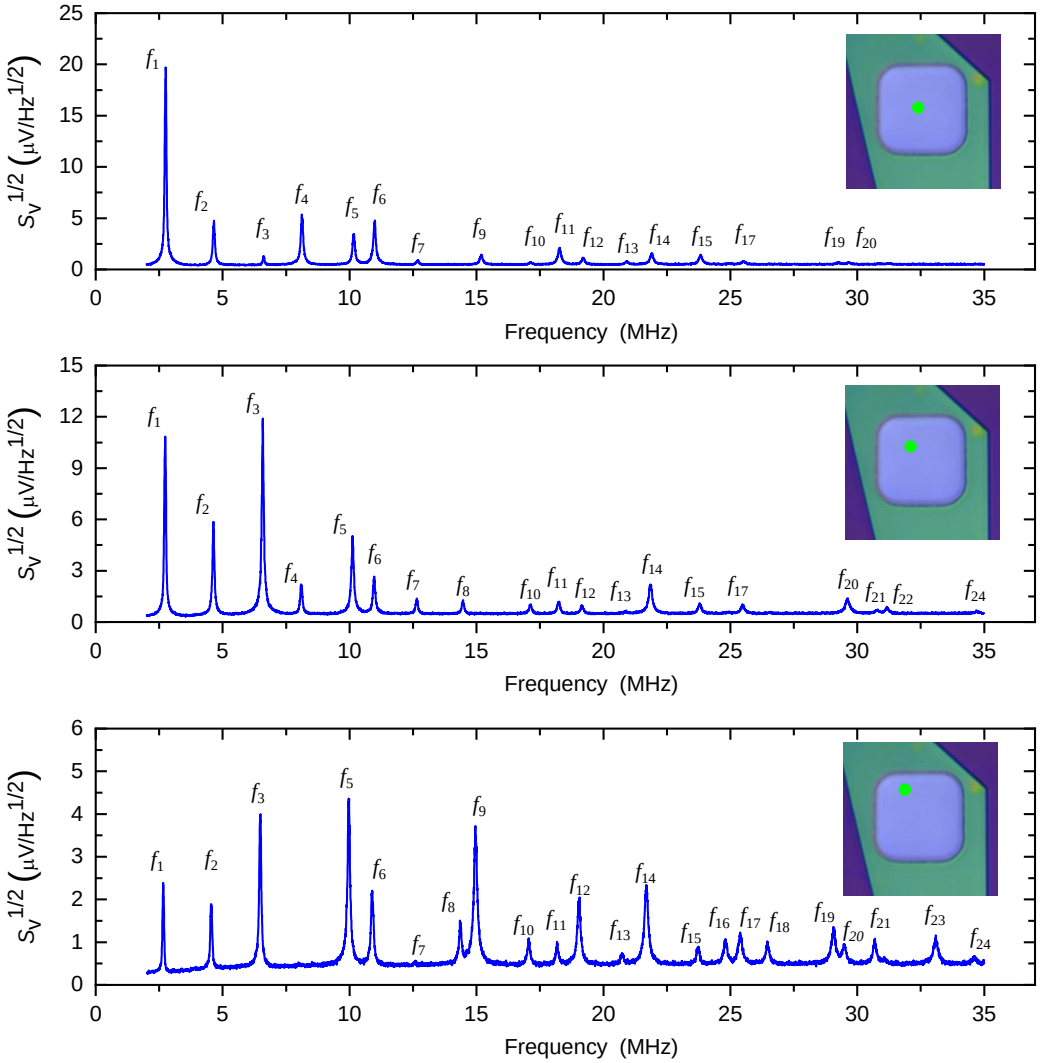

Fig. S10. Measurements of thermomechanical resonance in a device (73.4 nm thick). A total of 24 Brownian resonance peaks are identified from the noise spectra (3 shown here) taken at different locations on the device, with laser spot positions indicated by the inset optical images. Image sizes: 24.1 μm by 24.1 μm.

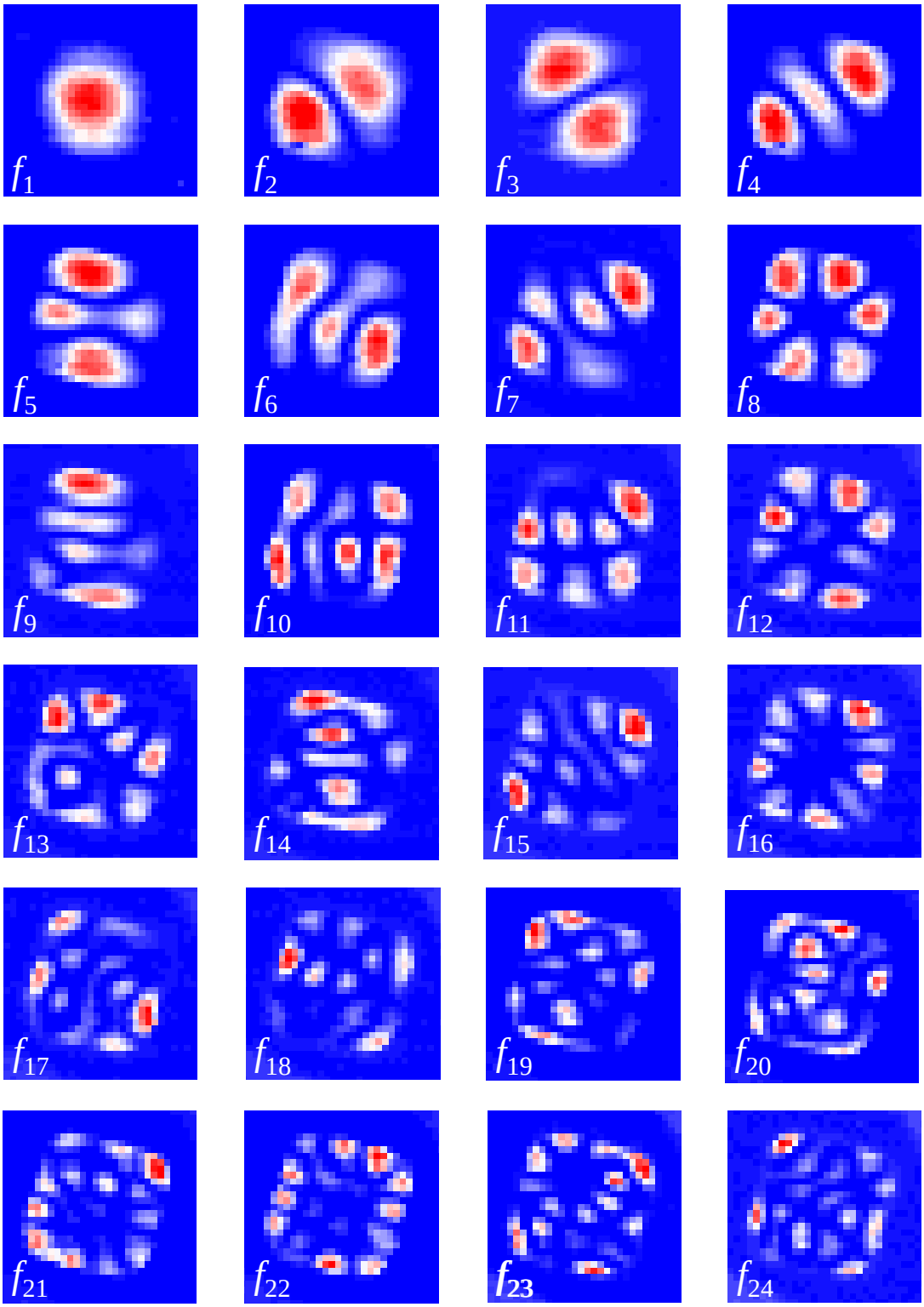

Fig. S11. Mapping of thermomechanical resonance in the same device (73.4 nm thick) shown in Fig. S10. The resonance measurement is performed using spectromicroscopy technique [60, 61]. The mode shapes correspond to the labeled modes in Fig. S10. Map sizes: 18.75 μm by 18.75 μm.